

# Spontaneously generated X-shaped light bullets

P. Di Trapani,<sup>1</sup> G. Valiulis,<sup>2</sup> A. Piskarskas,<sup>2</sup> O. Jedrkiewicz,<sup>1</sup> J. Trull<sup>1</sup>, C. Conti,<sup>3</sup> S. Trillo,<sup>3,4</sup>

<sup>1</sup>*INFM and Department of Chemical, Physical and Mathematical Sciences, University of Insubria, Via Valleggio 11, 22100 Como, Italy*

<sup>2</sup>*Department of Quantum Electronics, Vilnius University, Sauletekio al. 9, bldg. 3, LT-2040 Vilnius, Lithuania*

<sup>3</sup>*Istituto Nazionale di Fisica della Materia (INFM)-RM3, Via della Vasca Navale 84, 00146 Roma, Italy and*

<sup>4</sup>*Department of Engineering, University of Ferrara, Via Saragat 1, 44100 Ferrara, Italy*

(Dated: August 5, 2018)

We observe the formation of an intense optical wavepacket fully localized in all dimensions, i.e. both longitudinally (in time) and in the transverse plane, with an extension of a few tens of fsec and microns, respectively. Our measurements show that the self-trapped wave is a X-shaped light bullet spontaneously generated from a standard laser wavepacket via the nonlinear material response (i.e., second-harmonic generation), which extend the soliton concept to a new realm, where the main hump coexists with conical tails which reflect the symmetry of linear dispersion relationship.

PACS numbers: 03.50.De, 42.65.Tg, 05.45.Yv, 42.65.Jx

Defeating the natural spreading of a wavepacket (WP) is a universal and challenging task in any physical context involving wave propagation. Ideal particle-like behavior of WPs is demanded in applications, such as microscopy, tomography, laser-induced particle acceleration, ultrasound medical diagnostics, Bose-Einstein condensation, volume optical-data storage, optical interconnects, and those encompassing long-distance or high-resolution signal transmission. The quest for light WPs that are both invariant (upon propagation) and sufficiently localized in all dimensions (3D, i.e., both transversally and longitudinally or in time) against spreading "forces" exerted by diffraction and material group-velocity dispersion (GVD,  $k'' = d^2k/d\omega^2|_{\omega_0}$ ) has motivated long-standing studies, which have followed different strategies in the *linear* [1, 2, 3, 4, 5] and *nonlinear* [6, 7] regime, respectively.

In the *linear* case, to counteract material (intrinsic) GVD, one can exploit the angular dispersion (i.e., dependence of propagation angle on frequency) that stems from a proper WP shape. The prototype of such WPs is the X-wave [2], a non-monochromatic, yet non-dispersive, superposition of non-diffracting cylindrically symmetric Bessel  $J_0$  (so-called conical or Durnin [1]) beams, experimentally tested in acoustics [3], optics [4] and microwave antennae [5]. Importantly, in the relevant case of WPs with relatively narrow spectral content both temporally (around carrier frequency  $\omega_0$ ) and spatially (around propagation direction  $z$ , i.e. paraxial WPs), X-waves require *normally* dispersive media ( $k'' > 0$ ). In this case, a WP with disturbance  $E(r, t, z) \exp(ik_0z - i\omega_0 t)$  ( $k_0 \equiv k(\omega_0)$ ,  $r^2 \equiv x^2 + y^2$ ), has a slowly-varying envelope  $E = E(r, t, z)$  obeying the standard wave equation

$$\hat{L}(\omega_0) E = 0; \hat{L}(\omega_0) \equiv i\partial_z + \frac{1}{2k_0} \nabla_{\perp}^2 - \frac{k''}{2} \partial_{tt}^2. \quad (1)$$

Laplacian, where  $\nabla_{\perp}^2 = \partial_{rr}^2 + r^{-1} \partial_r$  is the transverse Laplacian, and we limit our attention to luminal WPs traveling at light group-velocity  $1/k' = dk/d\omega|_{\omega_0}^{-1}$  by

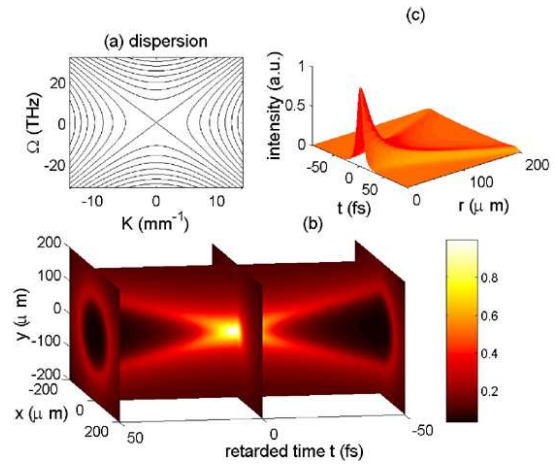


FIG. 1: Features of normally dispersive media ( $k'' > 0$ ): (a) spatio-temporal dispersion relation associated with paraxial wave equation (1); Different representations [(b) sections of color isointensity surfaces  $|E(x, y, t)|^2 = \text{const.}$ ; (c) intensity vs.  $r, t$ ] of a non-diffractive, non-dispersive linear X-wave ( $\Delta = 10$  fs,  $k'' = 0.02$  ps $^2$ /m,  $k_0 = 10^7$  m $^{-1}$ ).

introducing the retarded time  $t = T - k'z$  in the WP barycentre frame. Propagation-invariant waves  $E(r, t, z) = E(r, t, z = 0) \exp(i\beta z)$  can be achieved whenever their input spatio-temporal spectra  $E(K, \Omega, z = 0)$  lie along the characteristics of the dispersion relationship  $k''\Omega^2/2 - K^2/(2k_0) = \beta$ , which follows from Eq. (1) in Fourier space ( $K, \Omega$ ) ( $K$  is the transverse wavevector related to cone angle with  $z$ -axis  $\theta \simeq \sin \theta = K/k_0$ , and  $\Omega = \omega - \omega_0$ ). In the normal GVD regime ( $k'' > 0$ ) these curves, displayed in Fig. 1(a), reflect the hyperbolic nature of the wave equation (1) and show the common asymptotic spectral X-shape associated with the lines  $K = \pm 2k_0 k'' \Omega$  ( $\beta = 0$ ). When the spectral components lying along such X are superimposed coherently

(in phase), the field in the physical space  $(r, t)$  also retains a propagation invariant X-shape, as entailed e.g. by the exact solution  $E = \text{Re}\{[(\Delta - it)^2 + k_0 k'' r^2]^{-1/2}\}$  of Eq. (1) shown in Fig. 1(b-c). Here  $\Delta$  represents duration of the X-wave central hump. Main features of these waves are the conical (clepsydra) 3D structure and the slow spatial decay ( $1/r$  characteristic of  $J_0$  components [1]), displayed by Fig. 1(b) and (c), respectively.

Conversely, in the *nonlinear* (high intensity) regime, non-spreading WPs exploit the idea that, in self-focusing media, the nonlinear wavefront curvature can simultaneously balance the curvature due to diffraction and to GVD, combining features of spatial [9] and temporal [10] solitons to form a bell-shaped 3D-localized WP  $E(r, t)$ , so-called light-bullet [6]. In sharp contrast with X-waves, such compensation strictly requires *anomalous* GVD ( $k'' < 0$ ) [6], thus implying that along the WP tails, where Eq. (1) still holds true, space  $r$  and time  $t$  play the same role giving rise to strong WP localization [13]. Stable trapping, however, has been observed only in setting of reduced dimensionality (2D) [7, 8], including also other contexts, e.g. spin [11] or atomic waves [12] (3D kinetic energy and atom-atom attractive interactions act exactly as diffraction-GVD and self-focusing, respectively) where similar trapping mechanisms hold true.

In this work, we outclass the two approaches by demonstrating that *space-time localization in the normal GVD regime becomes accessible in the nonlinear regime*. Trapping is accomplished by mutual balance of intrinsic, shape-induced, and nonlinear contributions in a new type of WP, namely a nonlinear X-wave, which permits to get over two limitations at once. First, in contrast with linear X-waves, whose observation requires non-trivial input beam shaping [3, 4], our experiment reveals a remarkable "mode-locking" process that, starting from a conventional (gaussian) laser WP, spontaneously performs the reshaping into a localized X-shaped WP. Second, we believe this to be the first genuine nonlinear trapping in full-dimensional 3D physical space, since to date material and/or instability limitations [6, 7] have rendered the observation of light 3D bullets elusive.

Figure 2 describes the strong localization features observed after propagation in a 22 mm long sample of lithium triborate (LBO)  $\chi^{(2)}$  crystal. At the input we launch a laser WP at fundamental frequency (FF)  $\omega_0 = 2\pi c/\lambda_0$ ,  $\lambda_0 = 1060$  nm, with gaussian profile in both  $t$  (with FWHM duration in the 100–200 fs range) and  $r$  (45  $\mu\text{m}$  FWHM at waist, located few mm before the crystal so that the input beam is slightly diverging). The LBO crystal is tuned for generation of optical second-harmonic (SH) in the regime of relatively large positive phase mismatch  $\Delta k = 2k(\omega_0) - k(2\omega_0) = 30 \text{ cm}^{-1}$  or effective self-focusing for the FF beam [15]. When the input energy exceeds about 0.25  $\mu\text{J}$ , mutually trapped localized WPs at FF and SH are observed (see Fig. 2). Time-integrated measurements of spatial profiles (Fig. 2, top) indicate that diffraction is fully defeated to yield a spatial soliton-like beam [9], while temporal autocor-

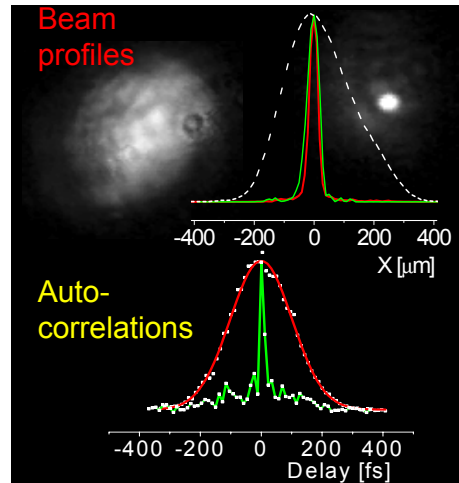


FIG. 2: Top: output transverse beam profiles in the linear (white) and nonlinear (green: SH; red: FF) regime. The diffracted (left) and localized (right) spots recorded at the output of the crystal are also shown. Bottom: temporal auto-correlation traces (collinear technique) showing the transition from the linear regime (red) to the compressed WP (green).

relations reveal a single pulse which is strongly compressed (down to  $\sim 20$  fs, see Fig. 2, bottom). Remarkably nonlinear mixing balances the two highest-order dispersive effects, namely the tendency of FF and SH to walk-off due to group-velocity mismatch (GVM)  $\delta V = k'(2\omega_0) - k'(\omega_0)$  and GVD, which act in the linear regime over characteristic length scales 50 and 2.5 times shorter than the crystal length, respectively. Relying on nonlinear scenarios known to date, the present result is unexpected. In fact, the normal GVD and the strong GVM of LBO do not allow an explanation in terms of light bullets, whereas the dynamics of self-focusing with normal GVD is dominated by pulse splitting without envisaging localization whatsoever [14].

In order to get a deeper understanding, we performed a set of numerical experiments by integrating the well-known model [15], which generalizes Eq. (1) to nonlinear coupling of envelopes  $E_m(r, t, z)$  ( $m = 1, 2$ , carrier  $m\omega_0$ )

$$\begin{aligned} \hat{L}(\omega_0) E_1 + \chi E_2 E_1^* \exp(-i\Delta kz) &= 0, \\ \hat{L}(2\omega_0) E_2 + \delta V \partial_t E_2 + \chi E_1^2 \exp(i\Delta kz) &= 0, \end{aligned} \quad (2)$$

In Fig. 3 (top) we show snapshots of the space-time evolution. It is clear that, in the first stage ( $z = 10$ –15 mm), the generation of light at SH is accompanied by strong self-focusing, in turn inducing pulse compression (in spite of the normal GVD that would cause temporal broadening of plane-waves). The WP becomes asymmetric since self-focusing is stronger where the SH, which lags behind because of GVM, tends to be. More importantly, during this process the WP undergoes a strong reshaping, where a large fraction of energy is radiated off-axis to form the tails of a conical wave (see snapshot at  $z = 20$  mm). After this stage, however, the collapse stops and the WP

propagates (locked with the SH) with immutable shape and nearly constant energy, duration, and size.

By changing the parameters in Eqs. (2) we can conclude that: (i) nonlinearity is the key element that drives the reshaping and holds the WP together. In fact, by switching it off after the transient (i.e.,  $\chi = 0$  for  $z > 20$  mm), the WP exhibits strong diffraction and extremely fast FF-SH walk-off. The reshaped WP can by no means be considered a linear X-wave; (ii) in our crystal, GVM is the dominant dispersion term affecting the asymptotic duration and width of the localized WP (both decrease for smaller GVM). However, (symmetric) X-shaped WPs are formed also in the ideal case of vanishing GVM, provided that GVD is normal; (iii) the WP reshaping strongly affects the phase modulation process, which reveals the contribution of an effective anomalous GVD; (iv) by including additional cubic nonlinearities [15], the phenomenon remains qualitatively unchanged.

A more rigorous ground for explaining the dramatic reshaping shown in Fig. 3 is offered by the investigation of two different aspects, both implicitly accounted for by Eqs. (2): (i) the stability of continuous plane-waves; (ii) the existence of nonlinear X-shaped eigen-solutions. Though somewhat idealized, the results of this analysis allow gathering the two basic features of the spatio-temporal dynamics, namely the transient reshaping of the input gaussian-like WP followed by the quasi-stationary regime.

The linear stability analysis of  $z$ -invariant solutions of Eqs. (2) with ideally vanishing spatio-temporal spectral width (i.e., continuous plane waves) always reveal the presence of exponentially growing weak (up to noise level) perturbations with definite frequency  $K, \Omega$ . However, the instability features reflect the symmetry of the linear wave equation, thus being qualitatively different in the normal and anomalous GVD regime, respectively. While anomalous GVD leads to narrow bandwidth features as in conventional spatial or temporal modulational instability [15], the hyperbolic structure of the diffraction-dispersion operator in the normal GVD regime of our experiment leads to exponential amplification of conical wave perturbations (Bessel  $J_0$  beams) with frequencies basically approaching the asymptotes of Fig. 1(a) [16]. When growing spontaneously from noise, the amplified components in the virtual infinite bandwidth (in reality limited by non-paraxiality and higher-order dispersion not accounted for in Eqs. (1-2)) leads to colored conical emission. Our calculations show that the phenomenon persists under dynamical conditions (unseeded SH generation) and when pumped by short-pulse narrow-beam inputs, as in our experiment. In the latter case, the amplification of proper frequency components of the WP preserves the mutual phase coherence, thus acting as a trigger which drives the transformation of the WP into the X-wave shown in Fig. 3. In other words, it is the conical instability that probes the symmetry of the underlying linear system in amplifying those components which allow both diffraction and dispersion of the whole

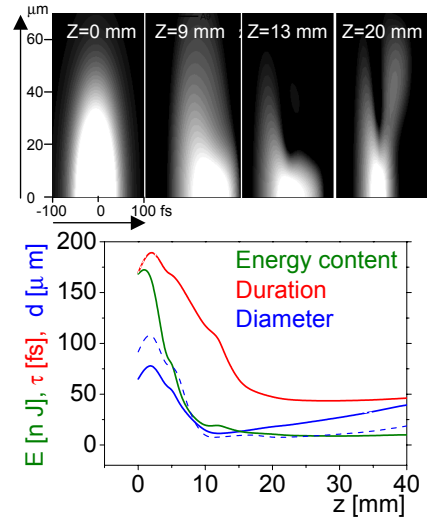


FIG. 3: Numerical simulation of the localization process observed in our LBO sample [from Eqs. (2) with  $k''(\omega_0) = 0.016 \text{ ps}^2/\text{m}$ ,  $k''(2\omega_0) = 0.089 \text{ ps}^2/\text{m}$ ,  $\delta V = 45 \text{ ps/m}$ ,  $\chi = 7 \times 10^{-5} \text{ W}^{-1/2}$  ( $d_{eff} = 0.85 \text{ pm/V}$ )] from an input gaussian WP with 45  $\mu\text{m}$  waist, 170 fs duration, and 0.26  $\mu\text{J}$  energy. Top: snapshots showing the FF beam in the  $t - x$  plane. Bottom: evolution of the beam diameter, duration, and energy content of main localized hump. The dashed line refers to more energetic (e.g., slightly wider and longer) input WPs for which even the small residual diffraction (solid line) is removed. In this case, however, the reshaping leads to higher peak intensity close to damage threshold of LBO.

WP to be removed.

A second, strong argument in favour of the nearly asymptotic character of the evolution shown in Figs. 3, is the existence of stationary localized solutions of Eqs. (2). We have recently shown, indeed, that the natural propagation-invariant [i.e., with dependence  $E_m(r, t) \exp(im\beta z)$ ,  $m = 1, 2$ ] localized eigensolutions of SH generation process in the normal GVD regime (either with or without GVM) are indeed nonlinear X waves [17]. These waves are similar to those shown in Fig. 1(b-c) except for the fact that their peak intensity is related to their duration and width through the nonlinearity.

Since the measurements in Fig. 2 give information only about the WP central hump, in order to confirm experimentally that the observed strong focusing and compression dynamics is indeed driven by the formation of an X-wave, we have performed different additional measurements. First, we have characterised the propagation of the WP in air after the LBO nonlinear crystal. We observe that the beam diffracts less than a gaussian beam of the same width (the divergence angle is 2.5 times less), and this net sub-gaussian diffraction witnesses a Bessel-like feature of the WP. Moreover, temporal broadening to 150 fs after only 10 cm of propagation in air is an indication that the WP develops strong angular dispersion. Both observations are in good quantitative agreement

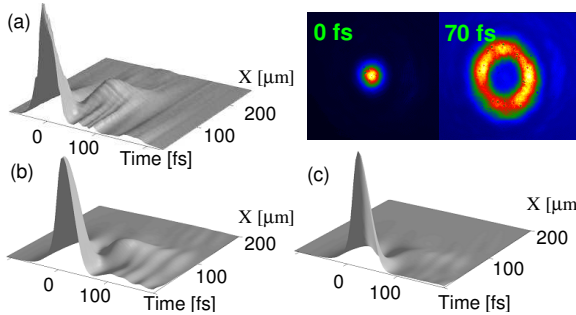


FIG. 4: (a) Output spatio-temporal intensity profile, as measured in air, 5 mm from the crystal output face. Insets: transverse intensity pattern in  $(x, y)$  plane measured at peak ( $t = 0$  fs) and with  $t = 70$  fs delay. (b) As in (a), numerical result from Eqs. (2). (c) As in (b) calculated right on crystal output.

with data obtained numerically from Eqs. (2). However, it is only the tomography of the output WP, i.e. mapping the WP intensity in space and time, that can give direct unequivocal evidence for the formation of an X-wave. To this end we have developed a new technique based on an ultrafast nonlinear gating, or a scanning cross-correlation technique, realized by frequency mixing the WP under investigation with a 20 fs, high contrast, steep front, probe pulse in the visible, which is uniform over a large (few  $\text{mm}^2$ ) area (the details of the set up will be presented elsewhere). Thanks to the high quality of the probe and the use of a very thin (20  $\mu\text{m}$ ) BBO mixing crystal, the apparatus has high temporal resolution. The intensity map of the output WP is reported in Fig. 4(a). The insets also show the measured beam profile in the transverse plane at time  $t = 0$  (peak) and  $t = 70$  fs (far from peak), respectively. The measured profile clearly shows the features of an X-wave with a

conical structure, which emanates from a strongly localized central spatio-temporal hump. Unlike conventional pulse splitting [14], here splitting occurs only sufficiently off-axis ( $x \sim 100\mu\text{m}$ ) in the WP low-intensity portion. For comparison we also report in Fig. 4(b) the profile calculated from Eqs. (2) under the same conditions, the agreement being excellent. The fringe-like structure that appears for large delays in both Fig. 4(a) and (b) is due to 5 mm of free-space propagation in air outside the crystal. Although the calculated profile on the output face of the crystal indeed shows that such fringes disappear [see Fig. 4(c)], measurement with perfect imaging on the output LBO face reveals saturation of the mixing process due to a too intense peak.

In summary, we have reported the first evidence that the natural 3D (temporal and spatial) spreading of a focused ultrashort wavepacket can be balanced in transparent materials at high intensity. The underlying mechanism is the *spontaneous* formation of a X-wave characterized by an intense (i.e., nonlinear) central hump self-trapped through mutual balance with (essentially linear) dispersive contributions associated with coexisting slowly decaying conical tails. While our experiment is carried out by exploiting self-focusing nonlinearities arising from quadratic nonlinearity, we envisage the general role that self-trapping mediated by nonlinear X-waves can have for a wide class of materials and applications encompassing centrosymmetric optical (Kerr) media [6], Bose-Einstein condensation [12], and acoustics [3].

We acknowledge support from MIUR (PRIN and FIRB projects), Unesco UVO-ROSTE (contract 875.586.2), Lithuanian Science and Studies Foundation (grant T-491), Secretaria de Estado y Universidades in Spain, and Fondazione Tronchetti Provera in Italy. We are grateful to the technical assistance of Light Conversion Ltd.

---

[1] J. Durnin, J.J. Miceli, and J.H. Eberly, Phys. Rev. Lett. **58**, 1499 (1987).

[2] E. Recami, Physica A **252**, 586 (1998); Salo, J. Fagerholm, A.T. Friberg, and M.M. Salomaa, Phys. Rev. Lett. **83**, 1171 (1999); J. Salo, J. Fagerholm, A.T. Friberg, and M.M. Salomaa, Phys. Rev. E **62**, 4261 (2000).

[3] J. Lu and J.F. Greenleaf, IEEE Trans. Ultrason. Ferrelec. Freq. contr. **39**, 441 (1992).

[4] P. Saari and K. Reivelt, Phys. Rev. Lett. **79**, 4135 (1997); H. Sönajalg, M. Rtsep, and P. Saari, Opt. Lett. **22**, 310 (1997).

[5] D. Mugnai, A. Ranfagni, and R. Ruggeri, Phys. Rev. Lett. **84**, 4830 (2000).

[6] Y. Silberberg, Opt. Lett. **15**, 1282 (1990); F. Wise and P. Di Trapani, Opt. Phot. News **13**, 28 (2002) and references therein.

[7] X. Liu, I.J. Quian, and F.W. Wise, Phys. Rev. Lett. **82**, 4631 (1999). X. Liu, K. Beckwitt, and F.W. Wise, Phys. Rev. Lett. **85**, 1871 (2000).

[8] H.S. Eisenberg, R. Morandotti, Y. Silberberg, S. Bar-Ad, D. Ross, and J.S. Aitchison, Phys. Rev. Lett. **87**, 043902 (2001).

[9] S. Trillo and W.E. Torruellas, eds., *Spatial Solitons* (Springer, Berlin, 2001).

[10] L. F. Mollenauer, R. H. Stolen, J. P. Gordon, Phys. Rev. Lett. **45**, 1095 (1980).

[11] M. Bauer, O. Buttner, S.O. Demokritov, B. Hillebrands, V. Grimalsky, Y. Rapoport, and A.N. Slavin, Phys. Rev. Lett. **81**, 3769 (1998).

[12] L. Khaykovich, F. Schreck, G. Ferrari, T. Bourdel, J. Cubizolles, L.D. Carr, Y. Castin, and C. Salomon, Science **296**, 1290 (2002); K.E. Strecker, G.B. Partridge, A.G. Truscott, and R.G. Hulet, Nature **417**, 150 (2002).

[13] Mathematically the strong localization is associated with existing solutions  $E(r, t) \exp(i\beta z)$  of Eq. (1) with  $k'' < 0$ ,  $\beta > 0$ , which decay *exponentially* in  $r, t \rightarrow \infty$ .

[14] J.K. Ranka, R.W. Schirmer, and A.L. Gaeta Phys. Rev. Lett. **77**, 3783 (1996).

[15] A.V. Buryak, P. Di Trapani, D. Skryabin, and S. Trillo, Phys. Rep. **370**, 63 (2002).

- [16] S. Trillo, C. Conti, P. Di Trapani, O. Jedrkiewicz, J. Trull, G. Valiulis, G. Bellanca, Opt. Lett. **27**, 1451 (2002).
- [17] C. Conti, S. Trillo, P. Di Trapani, G. Valiulis, A. Piskarskas, O. Jedrkiewicz, J. Trull, Los Alamos National Lab. e-print physics/0204066 (2002).